

# Excited-state photoemission with combined laser/synchrotron pulse excitation from C<sub>60</sub> chemisorbed on Ni(110)

T. Quast, R. Bellmann, B. Winter,<sup>a)</sup> J. Gatzke, and I. V. Hertel<sup>b)</sup>  
*Max-Born-Institut für Nichtlineare Optik und Kurzzeitspektroskopie, Postfach 1107,  
D-12474 Berlin, Germany*

(Received 11 July 1997; accepted for publication 20 October 1997)

Photoemission from C<sub>60</sub> chemisorbed on Ni(110) has been studied by one-photon photoelectron spectroscopy (1ppe) and two-photon photoelectron spectroscopy (2ppe) with synchrotron radiation (SR) and with synchronized SR and laser radiation. The 1ppe photoelectron spectra are studied as a function of C<sub>60</sub> coverage. Significant peak broadening relative to the thick film features is observed for the three leading valence bands. The large peak width of the valence levels obtained for the monolayer system is consistent with changes of the physical structure of C<sub>60</sub> due to the strong chemical interactions with the nickel substrate. The 2ppe experiment demonstrates transient excitation of the (*t*<sub>2u</sub>, *h*<sub>g</sub>) level of C<sub>60</sub>. © 1998 American Institute of Physics.

[S0021-8979(98)04703-3]

## I. INTRODUCTION

Two-photon photoemission (2ppe) pump/probe techniques using combined laser and undulator/synchrotron radiation are very promising for studying excited-state properties of adsorbate/surface systems. However, only a few experiments have been reported to date where laser/synchrotron pump/probe schemes have been attempted.<sup>1</sup> So far such experiments have primarily focused on the dynamics of photoexcited carriers (including space charge dynamics and surface recombination) in semiconductors.<sup>1</sup> In a more recent work the time-resolved photoemission from excitons in thick C<sub>60</sub> films has been studied using 5 ns pulses from a copper vapor laser ( $h\nu = 2.43$  eV) to populate states which are then probed by time-correlated 1 ns synchrotron pulses.<sup>2</sup> In the time-correlated 2ppe experiment for the C<sub>60</sub>/Ni monolayer system reported in the present work a picosecond laser pulse excites a normally unoccupied C<sub>60</sub> valence state above the Fermi energy  $E_F$ . A time-synchronized undulator pulse then ejects this transiently excited electron. To the best of our knowledge this is the first report of a coupled synchrotron/laser pulse experiment studying a molecular chemisorption system.

Our primary motivation for choosing the C<sub>60</sub>/Ni(110) system concerns an improvement to our understanding of the interaction of C<sub>60</sub> molecules with a metal substrate in general,<sup>3</sup> and nickel-catalyzed effects in particular.<sup>4-6</sup> Even though C<sub>60</sub> is by now agreed to form a chemical bond with many metal substrates,<sup>3,7-12</sup> which is argued to be more or less covalent in character, the details of this interaction are not well understood, e.g., the various amounts of shifting and broadening of the C<sub>60</sub> valence levels observed by the various spectroscopic techniques,<sup>3,7-12</sup> or even the occurrence of charge transfer (CT) from the metal into the C<sub>60</sub> lowest unoccupied molecular orbital (LUMO) for some metals can by no means be simply related to the metal workfunction. Also, the C<sub>60</sub>-metal binding energy is not known; only lower

bounds have been determined from thermal desorption studies which is due to the fact that C<sub>60</sub> molecules thermally dissociate before the C<sub>60</sub>-metal bond is thermally activated.<sup>13</sup>

From a more practical point of view, the C<sub>60</sub>/Ni(110) system offers a high density of occupied states (the nickel *d*-electrons) just at the nickel Fermi energy which is nearly aligned with the lowest unoccupied C<sub>60</sub> molecular orbital (LUMO *t*<sub>1u</sub>) for one monolayer (1 ML) C<sub>60</sub> on a metal substrate<sup>3,7-12</sup> (see below). Furthermore, even in its condensed phase C<sub>60</sub> exhibits very narrow valence bands due to the molecular character of solid C<sub>60</sub><sup>14-16</sup> which is rather advantageous for such a pump/probe experiment allowing an efficient and distinct optical absorption from near- $E_F$  (metal) states into empty C<sub>60</sub> molecular states above the LUMO. Finally, this system conveniently matches the available wavelength range of the Ti:sapphire laser system being used here (fundamental: 750–840 nm corresponding to 1.47–1.65 eV), roughly covering the LUMO *t*<sub>1u</sub>–*t*<sub>2u</sub>, *h*<sub>g</sub> gap (Ref. 9, and references therein). This situation is very different for high C<sub>60</sub> coverages where the lowest optical transition corresponds to the HOMO–LUMO spacing which is about 2 eV (Ref. 9, and references therein). This is too high an energy to be accessed by the fundamental wavelength of the laser and too low to match the laser second harmonic. In addition, the LUMO→*h*<sub>g</sub> transitions are symmetry allowed<sup>17</sup> while optical transitions between the HOMO and the LUMO in solid C<sub>60</sub> are only weakly allowed.

The paper is organized as follows: After a brief description of the experiment (Sec. II), we will first focus on the valence photoemission spectra as a function of the C<sub>60</sub> coverage and discuss the implications for the C<sub>60</sub>-nickel interactions for the monolayer system (Sec. III A). Then (Sec. III B) we will turn to the details of the laser pump and undulator-probe experiments for 1 ML C<sub>60</sub>/Ni(110).

## II. EXPERIMENT

The experiments were performed in an ultrahigh vacuum chamber (base pressure  $2 \times 10^{-10}$  Torr) equipped with a hemispherical electron energy analyzer (Omicron EA 125),

<sup>a)</sup>Electronic mail: bwinter@mbi-berlin.de

<sup>b)</sup>Also at Fachbereich Physik der Freien Universität Berlin.

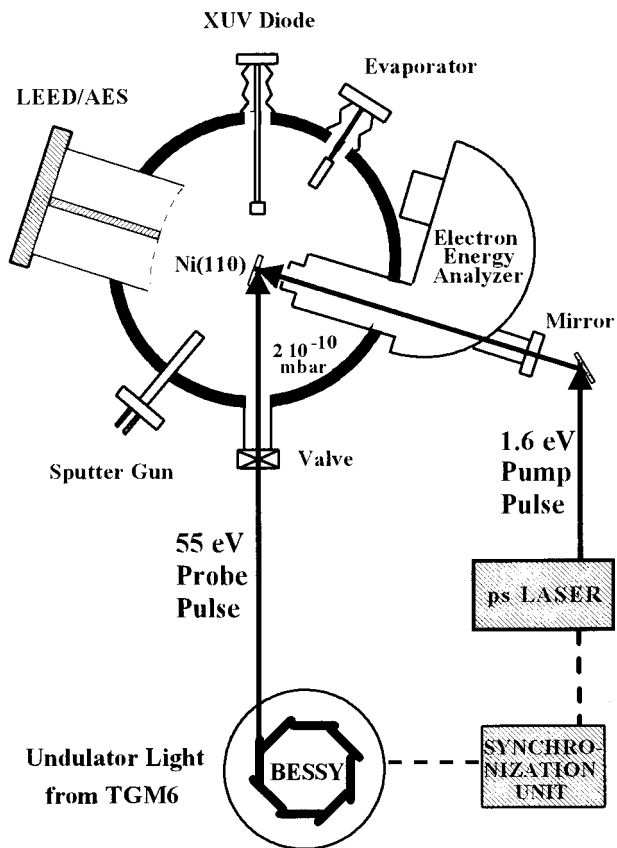


FIG. 1. Schematic experimental setup. The (pump) laser light is incident upon the Ni(110) crystal normal to the surface. The undulator radiation (probe) is incident on the sample at  $13^\circ$ . Photoelectrons are detected along the surface normal by a hemispherical electron energy analyzer. An XUV sensitive photodiode serves to control the temporal and spatial synchronization of the two pulses.

combined retractable four-grid low-energy electron diffraction/Auger electron spectroscopy (LEED/AES) optics, an ion sputter gun, a quadrupole mass spectrometer, an UHV evaporator, and a retractable photodiode sensitive in the vacuum ultraviolet, extreme ultraviolet and the soft x-ray spectral region (XUV) (Fig. 1).

The laser system (providing the pump pulse) used in the 2ppe experiment was a picosecond passively modelocked Ti:sapphire laser (Coherent Mira 900) pumped by an 8 W Ar-ion laser (Coherent Nova 200). The laser pulse width was 4 ps and the output power was  $>800$  mW in the 750–780 nm wavelength range. The unfocused laser light was incident normal at the crystal surface giving an irradiated spot size of ca. 2.5 mm diameter which corresponds to a power density of  $<5 \times 10^4$  W/cm<sup>2</sup>. The probe pulse was provided by undulator radiation (undulator periodicity of 70 mm) in single bunch mode at the TGM 6 monochromator at the Berlin electron storage ring for synchrotron radiation (BESSY). Typical photon densities were ca.  $10^5 - 10^6$  photons/pulse depending on the ring current. The undulator light was incident on the crystal surface at  $13^\circ$ . The photon energy was 55 eV (corresponding to an undulator gap of 53 mm) throughout the experiment. Time and spatial synchronization of the laser and synchrotron pulses were controlled by a silicon *p-n* junction XUV photodiode (IRD: AXUV-HS2) in combina-

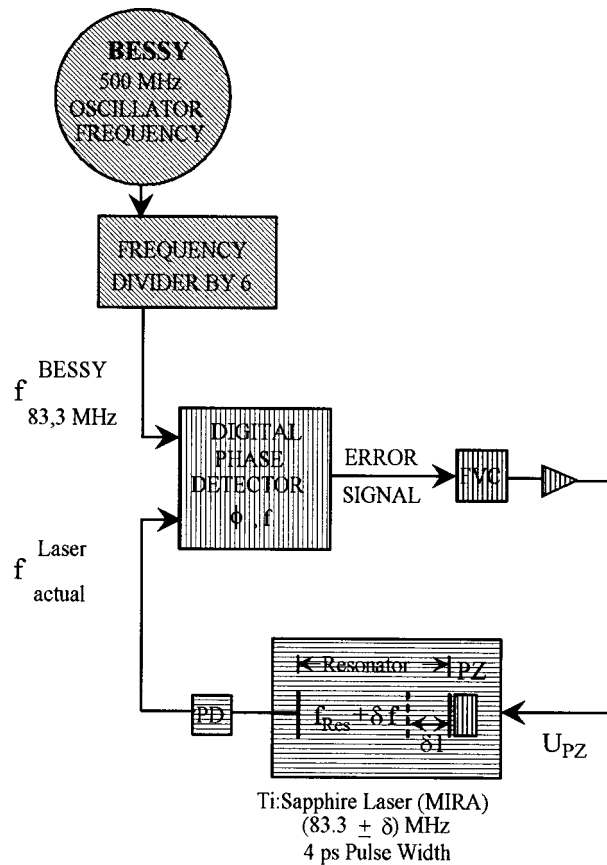


FIG. 2. PLL scheme for LR-SR pulse synchronization. A divider unit divides the BESSY 500 MHz ring frequency by six giving 83.33 MHz. The Ti:sapphire laser is set to the same frequency by suitably adjusting the resonator length. Frequency mismatch is compensated by the PLL fine adjustment. This is done by piezos driven by a circuit which compares both the input frequencies and phases (digital phase detector). The output piezo voltage  $U_{PZ}$  from a frequency-to-voltage converter is proportional to the mismatch (error signal).

tion with a 20 GHz sampling oscilloscope (Tektronix 1180). This particular photodiode had a rise time of 250 ps and a fall time of 2.5 ns.

The 500 MHz BESSY ring oscillator frequency was electronically divided by a factor of 6 (giving 83.33 MHz) in order to match the laser pulse frequency. Frequency and phase fine synchronization of the synchrotron (SR) and laser (LR) pulses is done by means of a homebuilt ‘‘phase locked loop’’ (PLL) (Fig. 2) which compensates for the frequency and phase mismatch by permanently adjusting the laser resonator length using a fast and a slow piezo. A digital frequency and phase detector (20 ps resolution) produces an error signal proportional to the mismatch which then is converted into a voltage to drive the piezos after amplification. The time constant of the loop is in the ms range as determined by the piezo/mirror frequency.

The actual character of the present *low resolution* synchronization as measured with the XUV photodiode (see above) is illustrated in Fig. 3. Figure 3(a) displays two synchrotron pulses (separated by 208 ns; single bunch) together with the laser pulses (separated by 12 ns corresponding to 83.33 MHz). In that example the laser pulse is delayed by 4 ns relative to the undulator pulse. The laser intensity had

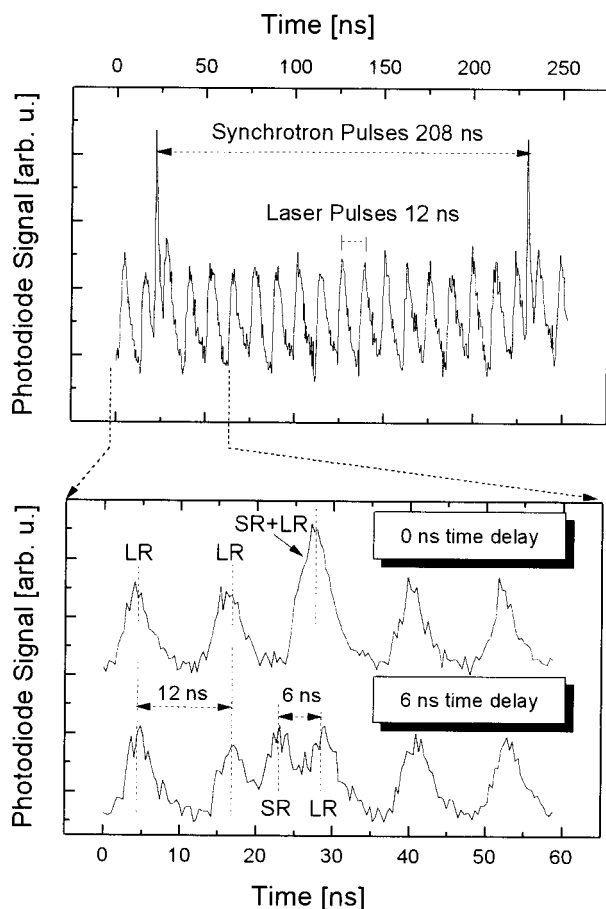


FIG. 3. Time-synchronized undulator (55 eV) and laser pulses (1.65 eV) recorded by a XUV photodiode for different delay times. (a) Two undulator pulses are displayed separated by 208 ns (corresponding to 4.8 MHz) together with the laser pulses separated by 12 ns (83.33 MHz); the time delay between undulator and the “first” laser pulse is 4 ns. (b) Blown up time scale; zero delay (top) and 6 ns delay (bottom) between undulator and laser pulse. Intensity is in arbitrary units. The laser signal has been attenuated in order to obtain comparable pulse heights. The large width of the recorded pulses is due to the slow response time of the XUV photodiode used here.

been suitably attenuated in order to obtain comparable laser and synchrotron pulse heights. The upper and lower panels in Fig. 3(b) correspond to zero delay and 6 ns delay, respectively, but displayed on an enlarged time scale. All these data were recorded with the monochromator set to 55 eV. Note that, due to the 2.5 ns decay time of the photodiode used, the measured pulse width of ca. 2.5 ns is considerably larger than the actual width of the undulator pulses (expected to be ca. 500 ps<sup>18</sup>).

This LR/SR synchronization scheme was initially developed for a gas phase time-resolved SR/LR experiment in the BESSY multi bunch mode<sup>19</sup> and has not been modified for the present single bunch purpose. This has the disadvantage that not every synchrotron pulse is synchronized with a laser pulse because the round trip time of a single bunch at BESSY is 208 ns, but the laser pulses every 12 ns. Only every third synchrotron pulse will be synchronized with a laser pulse [since  $(3 \times 208)/12$  is an integer]. For the present purpose we will see that this is just about acceptable but a more appropriate synchronization scheme for the laser and synchrotron pulses will have to be applied in the future. This

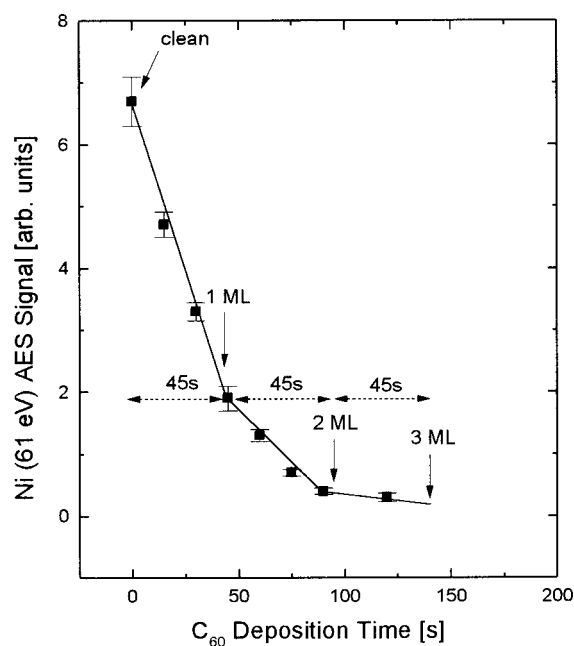


FIG. 4. Attenuation of the Ni-AES signal at 61 eV as a function of  $C_{60}$  deposition time on clean Ni(110) at room temperature. The arrows indicate the successive completion of the  $n$ th monolayer.

will be accomplished by electronically dividing the laser frequency (then set to 76.9 MHz) by a factor of 16 yielding 4.8 MHz which corresponds to the 208 ns round trip for the single bunch.

Photoelectrons were detected by an electron energy analyzer (EA 125; Omicron) to within  $\pm 8^\circ$  acceptance angle normal to the surface and the signal was recorded by counting electronics. For the current experiments the analyzer’s pass energy was set to 4 eV (constant energy mode) for the one-color experiment while we have used 8 eV for the 2ppe experiment in order to achieve a higher signal. This roughly corresponds to 100 and 150 meV resolution, respectively.

The Ni(110) single crystal (12 mm diameter; 2 mm thick) was attached to two horizontal tantalum wires ( $\Phi=0.3$  mm) which allowed resistive heating of the crystal. The sample could be rotated on axis ( $z$  axis) and translated in the  $xy$  plane. Sample cleaning was by repeated  $Ar^+$  sputtering cycles followed by annealing at ca. 1100 K. Sample cleanliness was routinely checked by AES and LEED. The  $C_{60}$  (purity >99%) deposited on the nickel surface was evaporated from an UHV evaporator at a temperature of ca. 630 K. Constant deposition rate was assured by means of a flux controller. During deposition the substrate was held at room temperature. The surface coverage as a function of  $C_{60}$  deposition time (at a given cell temperature) was estimated by monitoring the attenuation of the AES signal from Ni at 61 eV as illustrated in Fig. 4. This method is particularly useful if the growth proceeds layer-by-layer which is the case for  $C_{60}$  growth on nickel. The completion of an adsorbate layer is thus characterized by equally spaced, linear segments in the uptake plot (Fig. 4). Very similar results have been presented for  $C_{60}/Rh(111)$ .<sup>9</sup> Since the mean escape depth of 61 eV electrons is on the order of 10 Å this method is not applicable for fullerene surface coverages  $>3$  ML. Higher

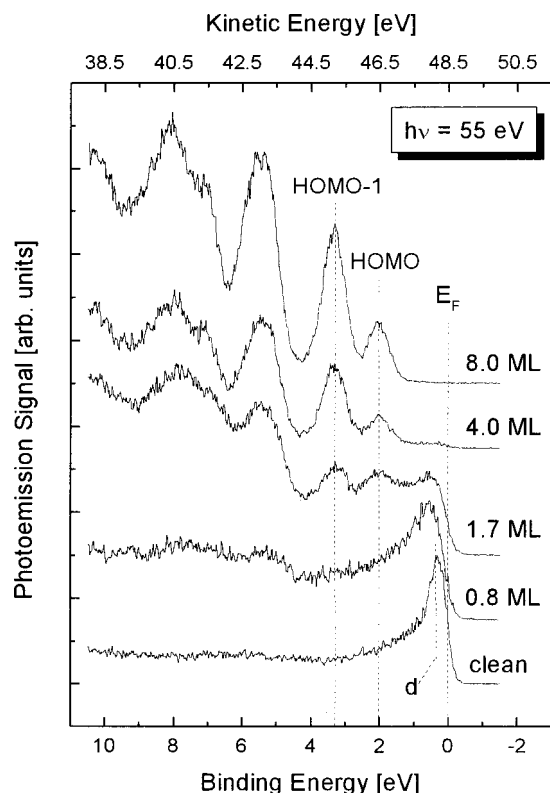


FIG. 5. PES from the clean Ni(110) crystal and for  $C_{60}$  coverages as indicated in the figure;  $h\nu = 55$  eV from the undulator. Peaks labeled HOMO, HOMO-1 refer to electron emission from  $C_{60}$ . Feature  $d$  is the nickel  $d$ -band emission. The FWHM of the HOMO and the HOMO-1 bands increases from 0.6 to  $>1.0$  eV for the 8 ML coverage and 1 ML coverage, respectively.

coverages have been estimated by linear extrapolation from low coverages which is valid assuming unit sticking probability. The AES signal from 1 ML coverage has been cross checked by suitably annealing a multilayer film: Due to the stronger (chemical) bonding of  $C_{60}$  to nickel as compared to the  $C_{60}$ - $C_{60}$  bonding<sup>5,9</sup> the multilayer system desorbs until a single monolayer of  $C_{60}$  remains. Under these conditions we also obtained the characteristic hexagonal LEED pattern of the  $C_{60}$  ordered monolayer.

### III. RESULTS AND DISCUSSION

#### A. One-photon photoemission: $C_{60}/Ni(110)$

Figure 5 displays the valence photoelectron spectra (PES) of  $C_{60}/Ni(110)$  as a function of the  $C_{60}$  surface coverage up to 8 ML. The energy scale is referenced to the (nickel) Fermi energy  $E_F$  which by definition corresponds to zero binding energy. All spectra were taken at 55 eV photon energy (from the single bunch undulator radiation). The labeling of the  $C_{60}$  levels follows the notation introduced in Refs. 14 and 15. For the clean surface we observe the  $d$ -band photoelectron emission from nickel only (peak labeled  $d$ ). The nickel Fermi edge, indicated by  $E_F$  lies 5.05 eV below the vacuum level for Ni(110).<sup>20</sup> Already at very low coverage the characteristic photoemission lines from  $C_{60}$  become visible, the first two arising from the HOMO  $h_u$  and HOMO-1  $g_g$ ,  $h_g$ , respectively, both of which are assumed

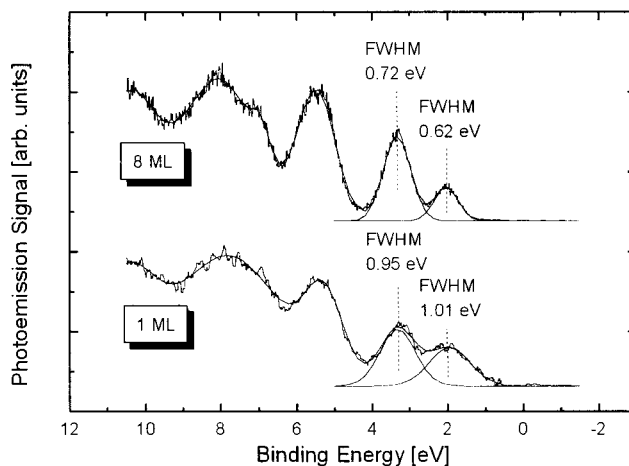


FIG. 6. Photoemission spectra for 1 ML  $C_{60}/Ni(110)$  (top), and for 8 ML  $C_{60}/Ni(110)$  (bottom) using  $h\nu = 55$  eV. The zero-coverage (bare) nickel spectrum has been subtracted from the top spectrum. The solid lines are fits to the data. There is a clear increase of the FWHM for the two leading valence bands for the monolayer system: 1.0 eV and 0.95 eV as compared to 0.6 eV and 0.7 eV for 8 ML  $C_{60}$ .

to have pure  $\pi$  character.<sup>14-16</sup> The latter is a pair of degenerate molecular orbitals. With increasing  $C_{60}$  adsorption the more strongly bound  $C_{60}$  valence electrons can also be clearly observed. They have mixed  $\pi$  and  $\sigma$  contributions. Note the complete attenuation of the nickel  $d$ -band emission for  $C_{60}$  coverages no larger than two to three  $C_{60}$  monolayers as a consequence of the electron mean-free path in  $C_{60}$  being on the order of one  $C_{60}$  layer,<sup>21</sup> which is consistent with the AES data presented in Fig. 4. This also explains why almost identical photoemission spectra are obtained for 8 ML and solid  $C_{60}$  films. Note that the low intensity ratio for HOMO-1 to HOMO (about 0.35 in the present 55 eV excitation experiment) is a consequence of the strong variation in the partial photoionization cross section for the outermost  $C_{60}$  valence orbitals. This is thought to result from electron interferences due to the formation of standing waves in the nearly spherical cage structure of the  $C_{60}$  molecule.<sup>22</sup>

There is a substantial broadening of the line widths of the two leading  $C_{60}$  valence features at low coverage which is increased by ca. 60% in comparison to the thick films. As shown in Fig. 6, the full width at half maximum (FWHM) of the HOMO and HOMO-1 band is about 0.6 eV for the 8 ML and  $>1.0$  eV at 1 ML coverage. (Note that in Fig. 6 the zero-coverage nickel spectrum has been subtracted from the 1 ML  $C_{60}$  spectrum.) This large absolute value of the FWHM for the monolayer system is consistent with strong  $C_{60}$ -metal interactions (see below). We observe no binding energy changes for the valence electrons as a function of coverage except a slight change in the peak shape of the feature at 8 eV binding energy. The HOMO- $E_F$  separation is 2.0 eV for all coverages. Possible LUMO band formation effects due to charge transfer (CT) from occupied metal states are entirely masked by the strong substrate  $d$ -band emission energetically coinciding with the  $C_{60}$  LUMO. We note that the above observations regarding the zero peak shift plus the peak broadening are rather unlikely to directly reflect the multilayer- $C_{60}$ -substrate interactions. In a most recent work

Maxwell *et al.*<sup>23</sup> have convincingly demonstrated that the valence peak shifts (relative to the substrate  $E_F$ ) observed for films thicker than ca. 2 ML  $C_{60}$ , on different metal substrates, largely reflect steady-state charging and screening effects consistent with the molecular character of solid  $C_{60}$  and are not due to the direct multilayer-metal interactions. The authors also address the resulting consequences for proper energy referencing of the measured multilayer features to either  $E_F$  or  $E_{vac}$ .<sup>23</sup> The zero binding energy shift (or missing shift) obtained in the present work is likely to result from three-dimensional growth patterns after the first monolayer is completed,<sup>24</sup> i.e., possible intrinsic shifts due to the multilayer- $C_{60}$  interactions would appear to be masked by islanding which averages over several coverages. Multilayer islanding may in fact be responsible for the somewhat larger FWHM obtained for our multilayer valence features as compared to the literature values.<sup>10,12</sup> This, of course, does not apply for the 1 ML system.

For comparison,  $C_{60}$  adsorbed on various other metal surfaces shows more or less pronounced shifts and/or broadening of the two leading valence bands. For instance, on Au(110) (WF=5.1 eV) the four leading valence features (except the second) are shifted by 0.9 eV to lower binding energies for the monolayer as compared to higher coverages which has been attributed to the  $C_{60}$  LUMO pinning at the metal Fermi level.<sup>10</sup> The HOMO is then located at ca. 1.7 eV (below the nickel  $E_F$ ), in contrast to 2.6 eV for the thick film. Note that 2.6 eV plus WF almost reproduces the ionization potential 7.6 eV of free molecular  $C_{60}$ .<sup>23</sup> This in turn brings the LUMO very close to  $E_F$  and LUMO mixing might occur. However, no new structure near  $E_F$  associated with a partially filled LUMO has been observed for an Au(110) substrate (also Ref. 8). The absence of a distinct LUMO-derived band has been attributed to additional metal-substrate interactions. Hybridization between the Au  $d$ -bands and the  $C_{60}$   $\pi$  levels has been inferred from that study.<sup>10</sup> Also for 1 ML  $C_{60}/Ag(111)$  [WF=4.6 eV] all the valence levels shift. The HOMO binding energy, e.g., increases steadily with coverage from 1.85 eV at 0.5 ML to 2.7 eV at 30 ML.<sup>11</sup> Even LUMO band formation effects due to CT from metal  $s$ - $p$  electrons into the  $C_{60}$  LUMO exist for the silver monolayer system. Band formation for 1 ML  $C_{60}/Ag(111)$  has been confirmed in another photoemission study, showing, however, negligible HOMO binding energy shifts as a function of surface coverage.<sup>8</sup> Confusingly, in the pioneering work of  $C_{60}$ -metal interactions no LUMO-derived band was observed for  $C_{60}/Ag$ .<sup>7</sup>

Surprisingly, the observed peak width for the  $C_{60}$ /nickel monolayer system appears to be very similar to the findings for aluminum and platinum substrates. The  $C_{60}/Al(111)$  {WF[Al(111)]=4.2 eV} monolayer system is characterized by particularly large broadening of the HOMO and HOMO-1 features, up to 1.2 eV for 1 ML  $C_{60}$ .<sup>12</sup> This is greater than any previously measured FWHM of the HOMO band for  $C_{60}$  monolayer systems but not too different from our present observations and from 1 ML  $C_{60}$  Pt(111).<sup>5</sup> Despite the low WF for Al which is smaller than for Ag and Cu no LUMO band formation due to CT occurs. Nor is there a LUMO effect observed for platinum. Generally such pronounced

broadening is interpreted as strong evidence of covalent bonding between adsorbate and substrate<sup>12</sup> involving changes in the physical structure of the  $C_{60}$  molecule which in turn lowers the degeneracy of the  $C_{60}$  electronic states.

From the above comparison with other monolayer systems we can conclude that the  $C_{60}$ -nickel interaction has a strong chemical character and manifests itself in a pronounced valence level broadening. The strong binding as such is not a surprising result for a transition metal. The interesting point here is the specific manifestation of this binding which differs from system to system, e.g.,  $C_{60}$  is also strongly chemically bound on a gold substrate having almost the same workfunction as nickel, but the peak broadening there is small while instead the energetic shift is pronounced. Again, one has to be careful about drawing meaningful conclusions from the multilayer "artificial" peak shifts.<sup>23</sup> Nonetheless, the current results once more demonstrate that different effects have to be accounted for in order to describe the complex binding interactions. This also applies to the existence of the LUMO-derived band which is obviously a result of some sensitive balancing between simple CT (back bonding) and molecular hybridization (HOMO-to-empty- $d$  band) effects. Unfortunately, the strong  $d$ -band emission near  $E_F$  in the present case precludes the actual observation of the LUMO band formation which would be very valuable in order to correctly interpret the  $C_{60}$ -nickel interactions. It is noted that based on a vibrational analysis, applying high-resolution electron energy-loss spectroscopy (HREELS),<sup>24</sup> ca. 2.3 electrons are transferred from the Ni(110) surface into each  $C_{60}$  molecule.

Strong chemical bonding of  $C_{60}$  to nickel has also been evidenced by the extreme stability of the 1 ML  $C_{60}/Ni(111)$  system upon high fluence pulsed laser light irradiation.<sup>6</sup>  $C_{60}$  molecules in direct contact to the nickel substrate survive internal temperatures up to ca. 3000 K due to very efficient dissipation of excitation energy from the adsorbate into the metal substrate on the time scale of the laser pulse width which was 20 ns. For comparison, decomposition of the free molecule is on the microsecond time scale at these temperatures.<sup>25</sup> A (catalyzed) decomposition of  $C_{60}$  molecules occurs only for laser fluences corresponding to transient surface temperatures above 3000 K. Considerably stronger bonding for  $C_{60}$  on Ni(110) as compared to noble metal surfaces has also been inferred from lattice strain arguments in a LEED study.<sup>24</sup> Furthermore, based on discrepancies between the charge states which have been obtained for the different  $C_{60}$  vibrational modes in HREELS it was also suggested that the adsorbed molecule is anisotropically distorted due to bonding with the nickel surface.<sup>24</sup>

## B. Laser/synchrotron 2ppe: 1 ML $C_{60}/Ni(110)$

Figure 7 gives a simplified schematic of the energy level diagram for the 1 ML  $C_{60}$ /nickel system, depicting the relevant states involved in our present two-color time-correlated 2ppe experiment. The solid lines in the left part of the figure represent the  $C_{60}$  occupied energy levels as obtained from the measured photoelectron spectra (Fig. 5). The energy scale corresponds to the measured binding energies

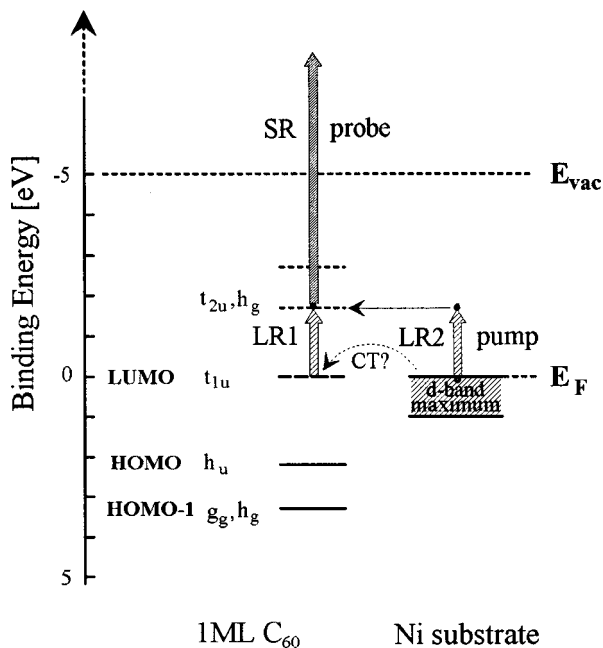


FIG. 7. Schematic energy level diagram for the 1 ML  $C_{60}/Ni(110)$  system. Left: Solid lines refer to occupied electronic states of  $C_{60}$ . Dashed lines represent normally unoccupied  $C_{60}$  states. The HOMO and HOMO-1 binding energies have been taken from Fig. 5 which justifies the LUMO-to- $E_F$  alignment. Right:  $E_F$  is the metal Fermi edge and the sketched  $d$ -band width corresponds to the maximum density of states. LR1 and LR2 represent optical transitions (by the laser pulse) into the  $C_{60}$  unoccupied  $t_{2u}, h_g$  bands from the partially filled (by CT from the substrate) LUMO  $t_{1u}$  and from the metal Fermi edge, respectively. SR indicates the ejection of electrons from these excited states into the vacuum by a 55 eV undulator-synchrotron pulse. WF is the Ni(110) workfunction (5.05 eV).

and illustrates the LUMO- $E_F$  alignment. For the 1 ML system the  $C_{60}$  features may be safely referenced to  $E_F$  as discussed above. Dashed lines refer to the energies of unoccupied  $C_{60}$  states which are only known for the solid film but are unknown for the 1 ML system under investigation. For simplicity, in Fig. 7 we have adopted the corresponding peak positions from the optical absorption spectrum of thick  $C_{60}$  films;<sup>26</sup> i.e., we have not attempted to account for possible polarization screening effects. Level labeling again follows the notation introduced in Ref. 15. The right part of the figure represents the metal energy level diagram together with the metal  $d$  band at maximum density of states.  $E_F$  is the nickel Fermi energy. The actual pump/probe experiment is represented by the vertical arrows indicating the absorption of a laser photon (LR) and the undulator (SR) excitation by which the transiently excited electron is ejected beyond the vacuum level. Two different laser pump channels denoted LR1 and LR2 may be principally distinguishable. LR1 corresponds to the direct excitation from the partially occupied  $C_{60}$  LUMO ( $t_{1u}$ ) into a higher normally unoccupied pair of states ( $t_{2u}, h_g$ )—which is an optically allowed transition. LR2 in Fig. 7 accounts for the possibility of the indirect population from resonance scattering into empty  $C_{60}$  states from metal  $d$  electrons incident upon the surface.

According to this simplified level picture the lowest optical transition  $t_{1u} \rightarrow t_{2u}, h_g$  is expected to begin near 1.6 eV (corresponding to the onset of the  $t_{2u}, h_g$  bands; center is

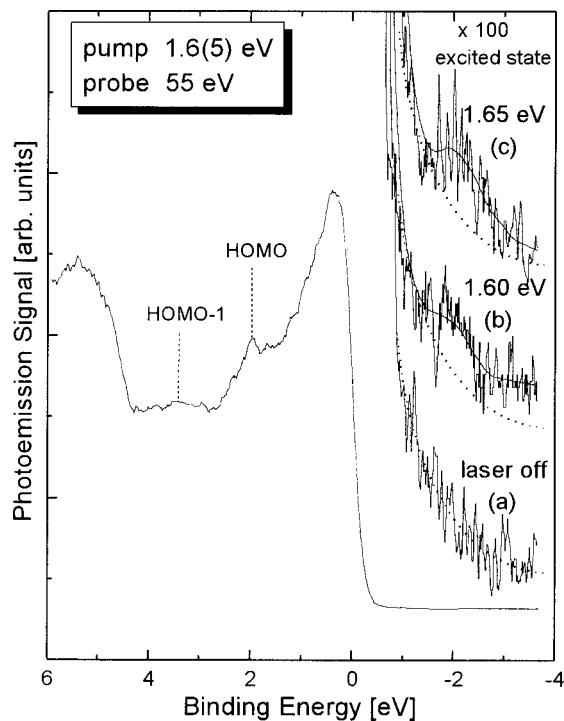


FIG. 8. Laser-excited valence photoemission spectrum from 1 ML  $C_{60}/Ni(110)$  for laser off (a), 761 nm (b), and 750 nm (c) excitation wavelength. The excited states were probed with 55 eV undulator pulses at zero time delay. Binding energy scaling is with reference to  $E_F$ . The new feature at  $E_F + 1.8$  eV is due to the ejection from the transiently occupied ( $t_{2u}, h_g$ ) bands as sketched in Fig. 7.

near 1.8 eV assuming zero level shifts). Hence, an extra peak in the PES centered at about  $E_F + 1.8$  eV may be expected to result when probing the laser-pumped surface by the time-correlated synchrotron pulse.

This is in fact consistent with our experimental observations shown in Fig. 8. The figure gives an expanded valence photoelectron spectrum (55 eV excitation) obtained for 1 ML  $C_{60}/Ni(110)$ , similar to the one displayed in Fig. 5. Different curves to the right of  $E_F$  correspond to different laser conditions. Spectrum (a) is the reference with the laser off. Clearly, a new feature near 1.8 eV above  $E_F$  appears in the PES when the pump laser is on and synchronized with the SR pulse. Two different laser wavelengths 761 nm [1.60 eV; (b)] and 750 nm [1.65 eV; (c)] have been used. The experiment has been reproduced several times. Note that the individual spectra have been displaced vertically by a constant offset with respect to each other. To guide the eye the baseline fit from case (a) is also shown in comparison with a fit (solid line) to the data in spectra (b) and (c).

The width of the extra feature is on the order of the one determined in Fig. 6 which shows that the new feature truly originates from the proposed transition. The fact that the +1.8 eV-band can be occupied using 1.6 eV photons clearly implies that either the  $C_{60}$  LUMO partially extends above  $E_F$  or that hot metal electrons are created thus considerably smearing out the Fermi edge.

We have also varied the time delay between the LR and the SR pulses such that the SR pulse arrives 1 ns and 2 ns after the LR pulse. For both these delays the 1.8 eV feature

was not observed. Although such a rapid relaxation would appear reasonable due to fast coupling to the metal substrate, we want to emphasize that the delay variation experiments have not yet been thoroughly cross checked. Hence we refrain at the present moment from communicating a relaxation time for the process under discussion. Note also that the question as to whether the  $C_{60} t_{2u}$ ,  $h_g$  band filling involves CT or an indirect process (see above) has to remain unanswered for the time being.

#### IV. CONCLUSIONS

We have studied the adsorbate system  $C_{60}$ -Ni(110) with one and two photon photoelectron spectroscopy. The investigation of the valence photoelectron spectra (1ppe) as a function of the  $C_{60}$  coverage revealed substantial broadening of the leading valence band features but constant binding energy (shifted by 0.6 eV with respect to the free molecule). These results are consistent with strong chemical interactions between the first  $C_{60}$  monolayer and the nickel surface. The multilayer-metal interactions, however, are difficult to quantify due to adsorbate charging effects which would require very thorough energy referencing. We have also demonstrated that the combination of time-synchronized laser and undulator-synchrotron pulses is a promising 2ppe technique for spectroscopy of unoccupied states of adsorbate/surface systems. Specifically, near- $E_F$  states of the 1 ML  $C_{60}$ /Ni(110) system were excited by 1.6 eV picosecond laser pulses into the normally unoccupied  $C_{60} t_{2u}$ ,  $h_g$  band. The excitation was detected by a time-synchronized 55 eV undulator pulse ( $t_{2u}$ ,  $h_g \rightarrow$  vacuum) which gave rise to a new feature in the PES at  $E_F + 1.8$  eV.

Even though the extra signal is still weak, due to the technical conditions detailed above, Fig. 8 clearly demonstrates that spectroscopy of laser-excited adsorbate states may be carried out using laser-pump/synchrotron-probe techniques on a picosecond time scale. A number of excitation schemes can now be envisaged which will make combined SR/LR a most promising experimental tool. To give just one more example, a SR pulse could be used to induce a high energy transition from an occupied core level into a normally unoccupied valence level (below  $E_{vac}$ ) of an adsorbate system which then is probed by a time-synchronized laser pulse. Such a scheme would open a realistic perspective to probe relaxation mechanisms after core level excitation in real time.

#### ACKNOWLEDGMENTS

This work was supported by the Bundesministerium für Bildung, Wissenschaft, Forschung und Technologie under

Contract No. 05 650BMA 6. The authors wish to thank M. Dose for developing the PLL synchronization electronics and E. E. B. Campbell for critically reading the manuscript.

- <sup>1</sup> See, e.g., review article by R. Haight, Surf. Sci. Rep. **21**, 275 (1995), and references therein.
- <sup>2</sup> B. S. Itchkawitz, J. P. Long, T. Schedel-Niedrig, W. R. Hunter, R. Schlögl, A. M. Bradshaw, and M. N. Kabler, *Proceedings of the International Conference on Physics of Semiconductors* (World Scientific, Singapore, 1995, ICPS22).
- <sup>3</sup> P. Rudolf, *Fullerenes and Fullerene Nanostructures*, edited by H. Kuzmany, J. Fink, M. Mehring, and S. Roth (World Scientific, Singapore, New Jersey, London, Hong Kong, 1994), p. 263.
- <sup>4</sup> T. Lill, H.-G. Busmann, B. Reif, and I. V. Hertel, Surf. Sci. **312**, 124 (1994).
- <sup>5</sup> C. Cepek, A. Goldoni, and S. Modesti, Phys. Rev. B **53**, 7466 (1996).
- <sup>6</sup> Ch. Kusch, B. Winter, R. Mitzner, A. Gomes Silva, E. E. B. Campbell, and I. V. Hertel, Chem. Phys. Lett. **275**, 469 (1997).
- <sup>7</sup> T. R. Ohno, Y. Chen, S. E. Harvey, G. H. Kroll, J. H. Weaver, R. E. Haufler, and R. E. Smalley, Phys. Rev. B **44**, 13 747 (1991).
- <sup>8</sup> S. J. Chase, W. S. Bacsa, M. G. Mitch, L. J. Pilione, and J. S. Lanin, Phys. Rev. B **46**, 7873 (1992).
- <sup>9</sup> A. Sellidj and B. E. Koel, J. Phys. Chem. **97**, 10 076 (1993).
- <sup>10</sup> A. J. Maxwell, P. A. Brühwiler, A. Nilsson, N. Martensson, and P. Rudolf, Phys. Rev. B **49**, 10 717 (1994).
- <sup>11</sup> G. K. Wertheim and D. N. E. Buchanan, Phys. Rev. B **50**, 11 070 (1994).
- <sup>12</sup> A. J. Maxwell, P. A. Brühwiler, S. Andersson, D. Arvanitis, B. Herdnäs, O. Karis, D. C. Mancini, N. Martensson, S. M. Gray, M. K.-J. Johansson, and L. S. O. Johansson, Phys. Rev. B **52**, R5546 (1995).
- <sup>13</sup> A. V. Hamza and M. Balooch, Chem. Phys. Lett. **201**, 404 (1993).
- <sup>14</sup> D. L. Lichtenberger, K. W. Nebesny, Ch. D. Rac, D. R. Huffman, and L. D. Lamb, Chem. Phys. Lett. **176**, 203 (1991).
- <sup>15</sup> P. J. Benning, D. M. Poirier, N. Troullier, J. L. Martins, J. H. Weaver, R. E. Haufler, L. P. F. Chibante, and R. E. Smalley, Phys. Rev. B **44**, 1962 (1991).
- <sup>16</sup> J. H. Weaver, J. Phys. Chem. Solids **53**, 1433 (1992).
- <sup>17</sup> See, e.g., S. D. Brorson, M. K. Kelly, U. Wenschuh, R. Buhleier, and J. Kuhl, Phys. Rev. B **46**, 7329 (1992); S. B. Fleischer, E. P. Ippen, G. Dresselhaus, M. S. Dresselhaus, A. M. Rao, P. Zhou, and P. C. Eklund, Appl. Phys. Lett. **62**, 3241 (1993), and references therein.
- <sup>18</sup> W. Anders, Ph.D. thesis, Universität Dortmund, Germany, 1992.
- <sup>19</sup> J. Gatzke, R. Bellmann, I. V. Hertel, M. Wedowski, K. Godehusen, P. Zimmermann, T. Dohrmann, A. v. D. Borne, and B. Sonntag, Nucl. Instrum. Methods Phys. Res. A **365**, 603 (1995).
- <sup>20</sup> H. B. Michaelson, J. Appl. Phys. **48**, 4730 (1977).
- <sup>21</sup> G. K. Wertheim, D. E. Buchanan, E. E. Chaban, and J. E. Rowe, Solid State Commun. **83**, 785 (1992).
- <sup>22</sup> Y. B. Xu, M. Q. Tan, and U. Becker, Phys. Rev. Lett. **76**, 3538 (1996).
- <sup>23</sup> A. J. Maxwell, P. A. Brühwiler, D. Arvanitis, J. Hasselström, and N. Martensson, Chem. Phys. Lett. **260**, 71 (1996).
- <sup>24</sup> M. R. C. Hunt, S. Modesti, P. Rudolf, and R. E. Palmer, Phys. Rev. B **51**, 10 039 (1995).
- <sup>25</sup> E. Kolodney, B. Tsipinyuk, and A. Budrevich, J. Chem. Phys. **100**, 8542 (1994); H. Hohmann, C. Callegari, S. Furrer, D. Grosenick, E. E. B. Campbell, and I. V. Hertel, Phys. Rev. Lett. **73**, 1919 (1994); B. Winter, R. Mitzner, Ch. Kusch, E. E. B. Campbell, and I. V. Hertel, J. Chem. Phys. **104**, 9179 (1996).
- <sup>26</sup> H. Ajie, M. M. Alvarez, S. J. Anz, R. D. Beck, F. Diederich, K. Fostiropoulos, D. R. Huffman, W. Krättschmer, Y. Rubin, K. E. Schriver, D. Senharna, and R. Whetten, J. Phys. Chem. **94**, 8630 (1990); J. P. Hare, H. W. Kroto, and R. Taylor, Chem. Phys. Lett. **177**, 394 (1991).